

## Article

# Research on Displacement Field of Soil around Pile with Different Density Based on Particle Image Testing Technology

Xiujie Zhang <sup>1,2</sup>, Hongzhong Li <sup>1,\*</sup>, Kaiyan Xu <sup>1</sup>, Zhanwu Ma <sup>3</sup>, Yonghong Wang <sup>4</sup> and Rongtao Yan <sup>5</sup><sup>1</sup> School of Civil Engineering, Guangdong Communication Polytechnic, Guangzhou 510650, China<sup>2</sup> Guangdong Province Communications Planning & Design Institute Group Co., Ltd., Guangzhou 510507, China<sup>3</sup> Civil Engineering College, North Minzu University, Yinchuan 750021, China<sup>4</sup> School of Civil Engineering, Qingdao University of Technology, Qingdao 266000, China<sup>5</sup> School of Civil Engineering, The Guilin University of Technology, Guilin 541000, China

\* Correspondence: lih001@gdcp.edu.cn

**Abstract:** Particle image testing technology has the advantages of non-intervention and high precision. In this paper, the particle image testing technology is combined with the indoor model test to explore the displacement development trend of the soil around the horizontal loaded pile under the difference of soil properties between layers. The principle of PIV technology is described, and the single-layer soil test group and the layered soil test group are set up, respectively. To this end, the indoor model test is carried out by changing the soil density. The study reveals that particle image testing technology can reduce the influence of data acquisition equipment on model tests in the maximum range, and restore the development trend of surface soil displacement in the horizontal load pile test to the greatest extent. Under the same load, the displacement influence area formed in front of and behind the pile of the two groups of tests takes the shape of a spindle centred on the pile body. The influence range of surface soil decreases with the increase of density. Moreover, the results of Tecplot analysis show that the soil stiffness is ranked from small to large as follows: single layer coarse sand, upper layer large particle size and lower layer small particle size test group, upper layer small particle size and lower layer large particle size test group, single layer fine sand. The test results can provide reference for the deepening of practical engineering.

**Keywords:** particle image testing technology; pile–soil interaction; horizontal load; layered soil; soil displacement field



**Citation:** Zhang, X.; Li, H.; Xu, K.; Ma, Z.; Wang, Y.; Yan, R. Research on Displacement Field of Soil around Pile with Different Density Based on Particle Image Testing Technology. *Buildings* **2022**, *12*, 2136. <https://doi.org/10.3390/buildings12122136>

Academic Editor: Ahmed Senouci

Received: 15 October 2022

Accepted: 28 November 2022

Published: 5 December 2022

**Publisher's Note:** MDPI stays neutral with regard to jurisdictional claims in published maps and institutional affiliations.



**Copyright:** © 2022 by the authors. Licensee MDPI, Basel, Switzerland. This article is an open access article distributed under the terms and conditions of the Creative Commons Attribution (CC BY) license (<https://creativecommons.org/licenses/by/4.0/>).

## 1. Introduction

Pile foundation has the characteristics of being able to pass through the soft soil layers to effectively transfer the load generated by the superstructure to the soil layer or rock layer with better engineering properties and higher bearing capacity. Therefore, it is widely used in high-rise buildings, port engineering, long-span bridges and offshore pile foundation platforms with strict requirements for bearing capacity and settlement. The design of pile foundation in these projects not only needs to meet the requirements of vertical bearing capacity, but also should focus on the influence of horizontal loads such as wind, wave hydraulics and occasional earthquakes on the stability of pile foundations during the service of the building structure. Pile–soil interaction under horizontal load is a complex form of action, which involves the change in mechanical responses of piles and soil under horizontal load.

At present, there are three main methods for studying the response of horizontal static pile–soil: the theoretical analysis method that reflects the action of pile–soil through a mathematical model, the experimental analysis method that obtains actual data through experiments, and the numerical simulation method. Based on the p–y curve theory of Matlock and Reese [1,2], the p–y curve method is constantly improving and developing.

Murchison et al. [3] put forward the tangent hyperbolic  $p$ - $y$  model under sand condition through practical case analysis, which is recommended by API for its convenient calculation and good continuity. In the aspect of experimental analysis, Zhang and Paul carried out research on the bearing characteristics of horizontal static pile foundation in cohesive soil, and explored the variation law of pile displacement, bending moment and soil resistance under the condition of cohesive soil [4,5]. Chen et al. [6] further studied the soil mechanical response of horizontal loaded piles in sand and cohesive soil foundations and analysed the influence of soil properties on pile-soil response.

Unfortunately, with the increase of pile diameter, the existing theory of the pile-soil  $p$ - $y$  curve model under horizontal load is not suitable for large diameter pile because it is based on small diameter and medium diameter piles as the research objects. It is difficult to study the response of horizontal load pile-soil interaction under large-diameter piles due to the lack of field tests on large-diameter piles and the lack of original data. Based on this, Alderlieste [7] carried out field tests on horizontal single piles with different pile diameters under the same sand conditions, and analysed and compared the influence of pile diameter on the bearing capacity and deformation characteristics of piles under the same horizontal load test conditions. The results show that the larger the diameter, the greater the stiffness of the pile-soil system under the same conditions. Further comparing the test results with the traditional horizontal load calculation formula, it is found that the traditional horizontal load calculation formula overestimates the initial stiffness of the soil.

Moreover, thanks to the great improvements in computing power, numerical analysis methods are more and more widely used in geotechnical engineering. Zhao et al. [8] used ABAQUS finite element software to analyse the strain of soil element around a three-dimensional horizontal loaded single pile. The results verified the existence of strain wedge, and analysed the influence of different horizontal loads and soil parameters on the parameters of wedge strain model.

However, the existing research ignores the stratification of natural soil in practical engineering, and only considers a single soil layer. Based on the previous research, the indoor 1 g test was used to carry out the corresponding model test of the horizontal loaded pile-soil system by changing the soil density and interlayer soil. Specifically, combined with particle image testing technology, the development trend of soil displacement around the surface pile was analysed.

## 2. Particle Image Velocimetry

### 2.1. Working Principle

Particle Image Velocimetry (PIV) is used to measure the deformation law of surface soil. The principle of PIV flow field measurement is to input a certain amount of tracer particles into the flow field first. The tracer particles are required to have good following and scattering properties, and will not cause any interference to the flow field. Then, the camera is used to take two consecutive pictures of the flow field measurement area, and obtain two particle images of the measured area at the same time. The displacement of the tracer particle in the time interval  $\Delta t$  between two photos is determined by the image cross-correlation analysis. The velocity of particles is calculated and processed in batches to obtain the velocity distribution vector diagram of the whole shooting flow field area [8,9]. Since the characteristics of sand can be recognised by CCD camera, the field change of soil mass on a two-dimensional plane can be directly measured without setting tracer particles, and then the displacement field contour map can be generated through post-processing.

### 2.2. Application of PIV Technology in Geotechnical Test

PIV technology was initially used in hydrodynamics and aerodynamics. The deformation of soil mass can be regarded as a process of low velocity flow, so PIV technology can also be applied to geotechnical test analysis to study the movement of micro soil particles [10–12]. Huang et al. used the traditional measuring point displacement method and PIV to measure the settlement of pile top and soil layer, respectively, in the nega-

tive friction model test of pile foundation. The analysis showed that the results obtained by the two methods were similar [13]. Secondly, PIV technology has the advantages of non-contact measurement and high measurement accuracy. In recent years, PIV technology has been widely used in geotechnical tests such as analysis of surface displacement field changes [14] and fracture evolution characteristics of rock materials after failure [15]. In the research on pile–soil interaction analysis and internal seepage observation of soil, Yuan et al. [16–18] designed a set of measurement systems combining transparent soil material and PIV technology. The system breaks through the traditional two-dimensional displacement deformation analysis and can intuitively explain the three-dimensional soil deformation problem.

To clearly understand the affected area of soil under external load and the development trend of soil under pile–soil interaction, the displacement field of sand particles on the soil surface under the lateral displacement of pile was obtained by importing the image taken during the test into PIVview2C software. The theoretical understanding of pile–soil interaction was further deepened by analysing the development law and influence radius of the displacement field. Then, the displacement field data were imported into Tecplot for post-processing work, and the displacement contour map was drawn. The research results from this work can provide reference for practical engineering.

### 3. Method and Materials

#### 3.1. Test Device and Model Pile

The indoor model test sandbox, whose four sides and bottom surfaces are made of acrylic glass plate material, is a cuboid container without a top surface. The thickness of the glass plate is 10 mm, and the internal size of the container is 36 cm × 24 cm × 50 cm (length × width × height). According to the similar proportional relation, the model pile is hollow aluminium alloy circular pile with length of 450 mm, diameter of 30 mm and wall thickness of 2 mm; its bending stiffness is 2429.8 N·m<sup>2</sup> and elastic modulus is 68 GPa. The embedded depth of single pile is 36 cm, and the sand cushion is 10 cm. Preloading holes are set 3 cm below the pile top.

During the test, the sand box was fixed on the reaction frame. After the sand cushion was laid, the pile was placed vertically in the centre of the model box to ensure that the pile moves on the two-dimensional plane. The test device is shown in Figure 1.

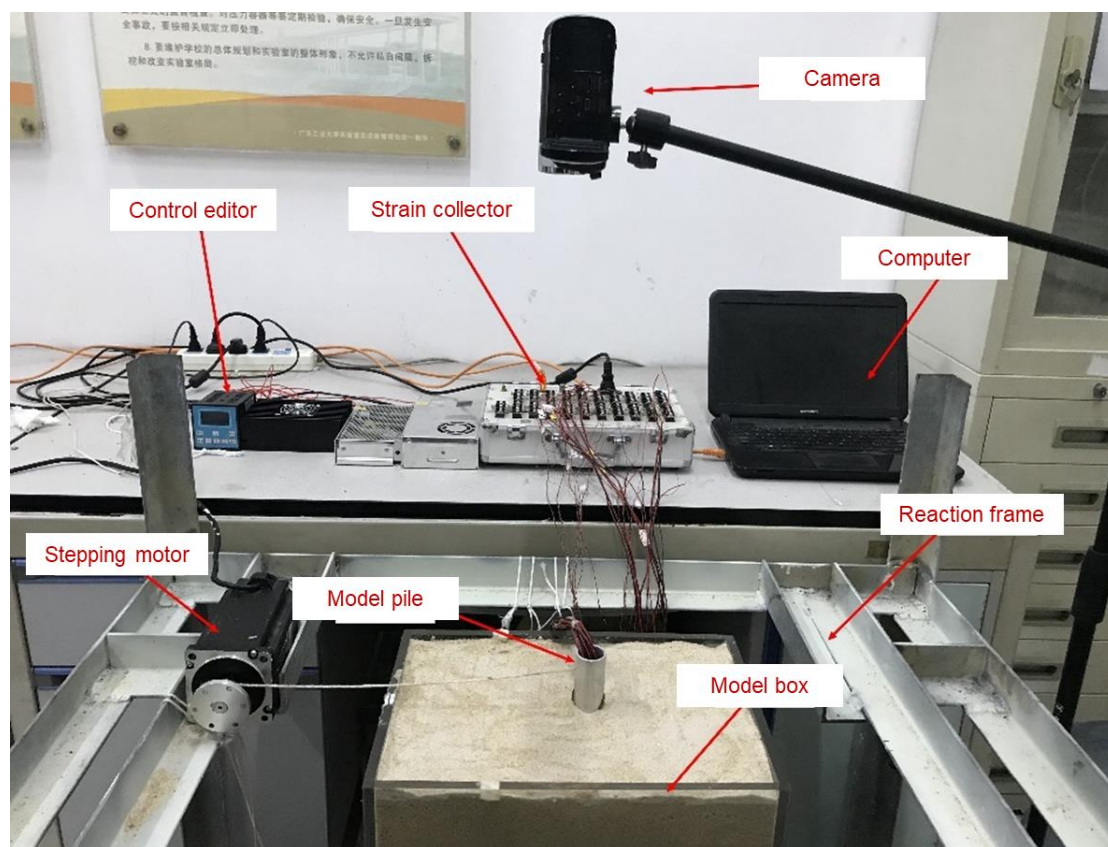


**Figure 1.** Test Platform.

### 3.2. Test Material

Fujian standard sands with different particle sizes ( $d = 0\text{--}1$  mm and  $d = 1\text{--}2$  mm) were used in this experiment. According to the specification [19], the specific gravity test, relative density test and particle gradation analysis test were carried out on the soil with two particle sizes. The non-uniformity coefficient of the Fujian standard sand was 5.29 and the non-uniformity coefficient was 1.05. The indexes of the test sand obtained from the test are shown in Table 1.

**Table 1.** Physical parameters of test sand.

Particle Size Range (mm)	Specific Gravity	Minimum Dry Density ( $\text{g}/\text{cm}^3$ )	Maximum Dry Density ( $\text{g}/\text{cm}^3$ )	Minimum Void Ratio	Maximum Void Ratio
0–1	2.64	1.43	1.88	0.40	0.85
1–2	2.64	1.43	1.75	0.50	0.85

In order to ensure the uniformity of the filling sand and achieve the relative density required for the test, the method of layered filling sand was adopted, and the thickness of each layer of filling sand was uniformly controlled to 4.5 cm. The electronic balance was used to weigh the quality of the filled layer of soil, and then the sand was evenly filled into the model box through the funnel to ensure that the height of the sand was flush with the scale line, to ensure that the density of the test met the requirements. Finally, filling to the pile buried depth of 36 cm corresponding to the scale line when the filling is stopped, the soil rested for 6 h before the test.

### 3.3. Data Acquisition and Analysis

The pile strain was collected by a Donghua strain acquisition instrument (DH3818N-2) during the test. The pile top displacement and soil displacement were measured by a high-definition camera placed 50 cm above the pile top. Before the test, the height and position of the bracket were first adjusted to ensure that the camera was at a height of 50 cm above the top of the pile. This height ensured that the camera shooting area could cover the entire test area. Wireless Bluetooth technology was used to take the picture so as to avoid the influence of camera disturbance on the test data. During the horizontal load loading process, the displacement was terminated from the initial position to the displacement loading. The displacement of the pile top and the soil was recorded according to the shooting frequency of once per second, and then the test image was imported into PIVview2C to analyse the soil displacement field.

### 3.4. Test Scheme

The horizontal load applied in this model test was provided by a stepper motor, and the loading rate was 0.083 cm/s. One end of the high-strength fibre nylon rope was fixed in the preload hole of the model pile, and then the other end was fixed on the drive shaft of the motor. The preload hole was kept highly consistent with the drive shaft of the motor, so as to ensure that the applied load was horizontal load.

This experiment was divided into two parts. Group A was to study the interaction mechanism of single-layer soil pile under different densities. The single-layer sand test was divided into model tests with particle size  $d = 0\text{--}1$  mm and  $d = 1\text{--}2$  mm. In order to study the influence of bearing sand pile–soil system under different densities, group B was divided into upper small particle size ( $d = 0\text{--}1$  mm), lower large particle size ( $d = 1\text{--}2$  mm), upper large particle size ( $d = 1\text{--}2$  mm), and lower small particle size ( $d = 0\text{--}1$  mm) model tests. In group B, the upper soil thickness of the layered soil test group was 27 cm and the lower soil thickness was 9 cm. The specific test groups are shown in Table 2.

**Table 2.** Test groups.

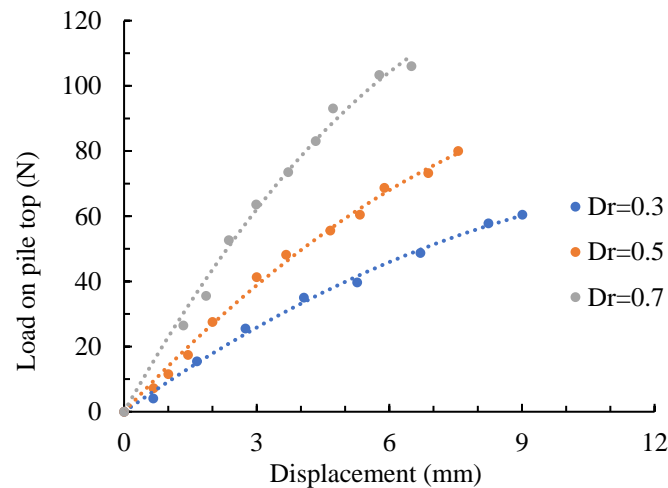
Test Group	Soil Layer Information	Soil Density ( $D_r$ )
Group A: Single Layer Soil	$d = 0\text{--}1$ mm	0.3
	$d = 1\text{--}2$ mm	
Group B: Layered Soils	$d = 0\text{--}1$ mm (Upper Layer)	0.5
	$d = 1\text{--}2$ mm (Lower Layer)	
	$d = 1\text{--}2$ mm (Upper Layer)	0.7
	$d = 0\text{--}1$ mm (Lower Layer)	

## 4. Results and Discussion

### 4.1. Analysis of Load Displacement Curve of Pile Top

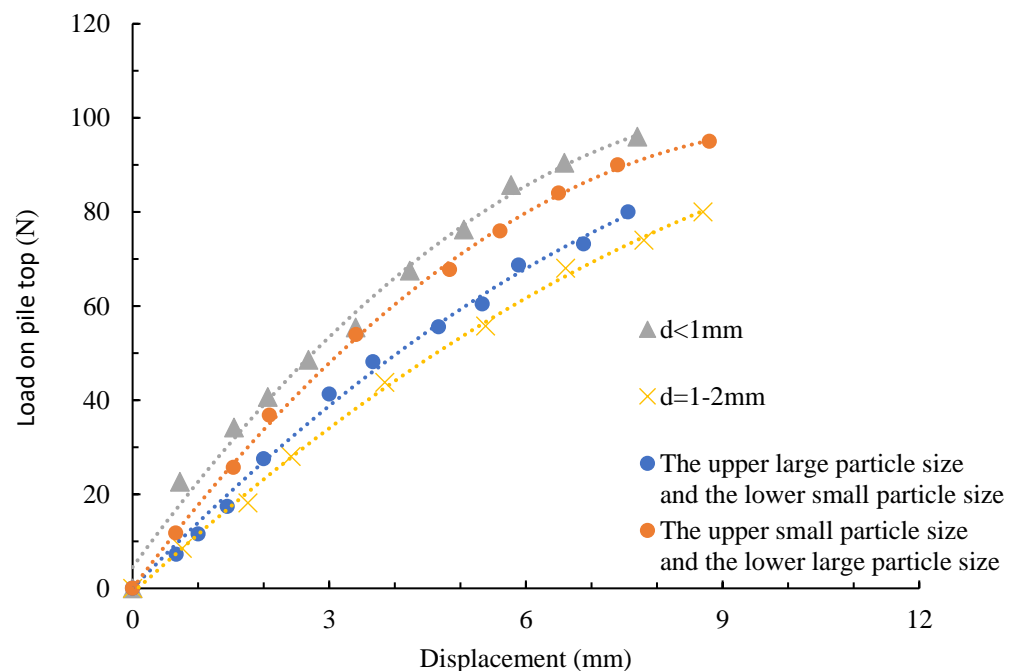
In the analysis of the pile–soil interaction of horizontally loaded piles, the degree of interaction between the pile and the soil around the pile with the load application process can be revealed through the analysis of the load displacement curve at the top of the pile, and the change in soil stiffness can be analysed through the increase of the slope of the curve.

Figure 2 shows the pile top load displacement relationship curve of the upper layer with small particle size and the lower layer with large particle size under the conditions of 0.3, 0.5 and 0.7 relative compactness, respectively. It can be seen from Figure 2 that there is a positive correlation between the pile top load and the displacement. With the increase of the load, the pile top displacement increases accordingly. Secondly, under the same pile top load, the pile top displacement values under the corresponding compactness conditions are in the order of 0.3 compactness, 0.5 compactness and 0.7 compactness, which indicates that the increase of compactness further limits the lateral displacement of the pile.



**Figure 2.** Pile top load displacement curve of upper small particle size and lower large particle size under different compactness.

As the pile top load displacement curves of different soil layers with different compactness are similar, this paper gives a comparison of pile top load displacement curves of different soil layers with 0.3 compactness. It can be seen from the curve that the development law of the load-displacement curve of single layer sand and layered sand is consistent in the early stage of loading, showing linear characteristics [20,21]. It shows that the sand in the loading stage is in elastic state, and then the difference appears with the continuous loading. The pile top load displacement curve can reflect the stiffness of the pile–soil system. From the pile top load displacement curve in the Figure 3, the stiffness of the single layer of small particle size sand is the largest, and the stiffness of the single layer of large particle size sand is the smallest. The middle is the layered soil test group; specifically, the stiffness of the upper layer of small particle size and the lower layer of large particle size test group is greater than the upper layer of large particle size and the lower layer of small particle size test group.



**Figure 3.** Pile top load displacement curve of different soil layers under 0.3 compactness.

#### 4.2. Displacement Field Analysis of Single Layer Soil

The displacement image of the surface soil when the pile top load was loaded to 30 N is studied. The image taken after loading to 30 N and the image without loading were imported into PIV software. Figure 4a–f is the particle displacement vector diagram of the single layer with small particle size and single layer with large particle size under three densities corresponding to 30 N load, respectively. The red vector displacement arrow parallel to the loading direction on the pile side in the drawing is the displacement of the conductor, which is interference displacement because the conductor also exists in the analysis area.

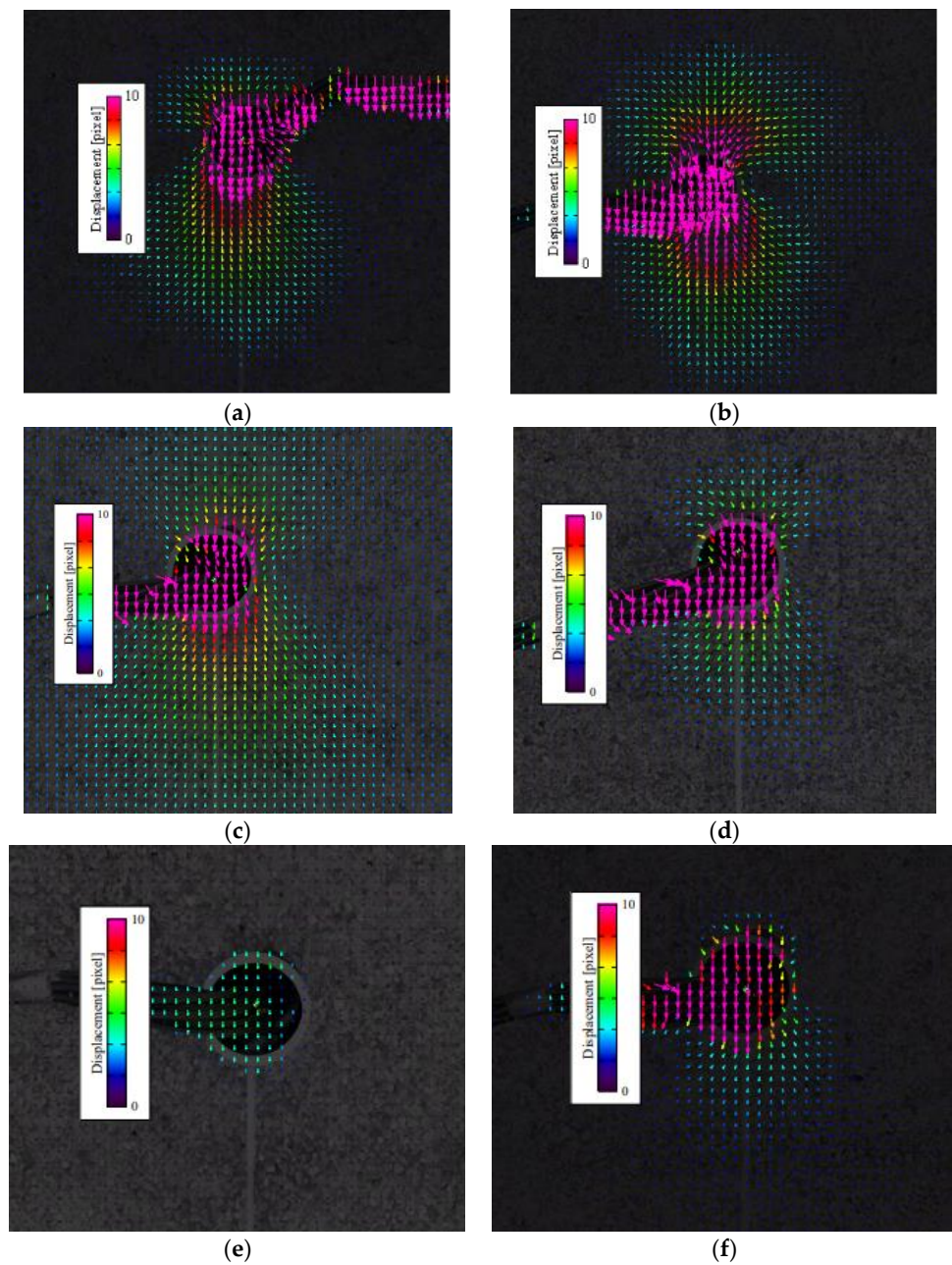


**Figure 4.** PIV images of single layer sand under different densities. (a)  $D_r = 0.3$  and  $d < 1$  mm; (b)  $D_r = 0.3$  and  $d = 1\text{--}2$  mm; (c)  $D_r = 0.5$  and  $d < 1$  mm; (d)  $D_r = 0.5$  and  $d = 1\text{--}2$  mm; (e)  $D_r = 0.7$  and  $d < 1$  mm; (f)  $D_r = 0.7$  and  $d = 1\text{--}2$  mm.

It can be seen from Figure 4 that the displacement of the surface sand particles does not only occur in the soil in front of the pile, but also in a certain range behind the pile. The size of the area is related to the particle size of the soil and the density of the soil. Under the horizontal load, the larger displacement mainly occurs in the loading centre area. Then, as the distance from the loading centre increases, the effect of the load on the surface sand gradually decreases, thus showing a decrease in the displacement value. The displacement trend of the sand particles is to diffuse into a spindle-shaped displacement influence area on both sides with the pile as the centre. Under the same load, the larger the density, the smaller the area of the displacement influence area. In addition, through the comparative analysis of small particle size sand and large particle size sand, it can be seen that the displacement influence area is also related to the nature of the soil. The overall performance is that the displacement influence area corresponding to the small particle size is smaller than that of large particle size sand, which also shows from the side that the stiffness of single layer small particle size sand is greater than that of large particle size sand, so its resistance to deformation is greater, so the displacement affected area is smaller under the same load conditions.

In order to further understand the size of the displacement influence area of the displacement field of the soil around the pile, and quantitatively analyse the displacement of the sand surface particles under the horizontal load of 30 N, the image displacement data generated by PIV are imported into Tecplot software to draw a more intuitive data chart (Figure 4). In Figure 4, the x-axis represents the width direction of the model box, and the y-axis represents the length direction of the model box, in mm. The coordinate origin is the centre position of the model box and the centre point of the pile body.

Comparing the range of 0.5 mm displacement isosurface in front of pile under different densities, it is found that the influence range decreases with the increase in density. The analysis shows that the decrease of the surface range is due to the increase in the density, which enhances the occlusion between the particles, so that the static friction force of the sand particles in front of the pile increases and resists the deformation caused by the external load. The soil behind the pile overcomes the effect of gravity after the density is improved, which puts the soil in a relatively stable state and leads to a decrease in the range of displacement isosurface.

It can be found from Figure 5a,b that, under the condition of 0.3 density, when the load on the top of the pile is 30 N, the maximum displacement of the sand surface of the single-layer small particle size test group is 2.8 mm, while the single-layer large particle size is 4.1 mm, indicating that under the same load, the stiffness of the small particle size sand is larger and the displacement is smaller. Similarly, under the density of 0.5 and 0.7, the maximum displacement values of sand surface in small particle size soil are 1.53 mm and 0.76 mm, respectively, while the maximum displacement values in large particle size soil are 2.61 mm and 1.37 mm, respectively. It can be concluded that the increase in soil density results in the increase of soil stiffness to obtain a higher ability to resist lateral deformation.

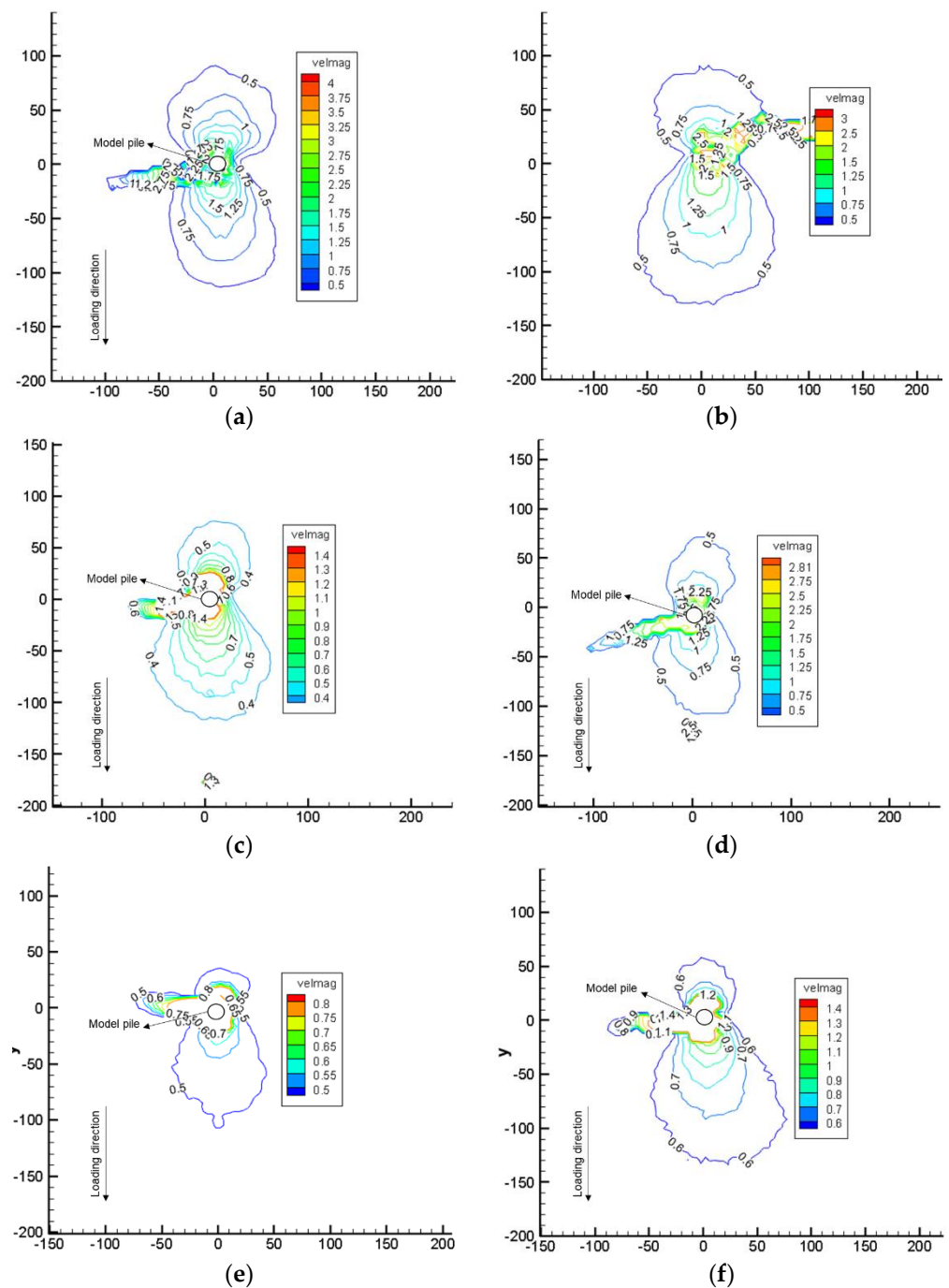


**Figure 5.** Displacement field analysis of single-layer sand under different densities. (a)  $D_r = 0.3$  and  $d < 1$  mm; (b)  $D_r = 0.3$  and  $d = 1\text{--}2$  mm; (c)  $D_r = 0.5$  and  $d < 1$  mm; (d)  $D_r = 0.5$  and  $d = 1\text{--}2$  mm; (e)  $D_r = 0.7$  and  $d < 1$  mm; (f)  $D_r = 0.7$  and  $d = 1\text{--}2$  mm.

#### 4.3. Displacement Field Analysis of Layered Soil

Figure 6 shows the displacement vector diagram of sand surface particles caused by horizontal load under three densities in the upper large particle size and lower small particle size test group, and the upper large particle size and lower small particle size test group, under 30 N load. From the PIV displacement diagram in the diagram, it can be gathered that the displacement movement trend between the particles on the soil surface of the layered soil test group is similar to that of the single-layer sand test group, which is manifested as a spindle-shaped displacement influence area centred on the pile body in front of and behind the pile. It can be observed that, during the horizontal load single pile

test, the particle displacement trend on the sand surface is basically similar, but the size of the displacement influence area is related to the density of the soil layer and the nature of the soil layer.

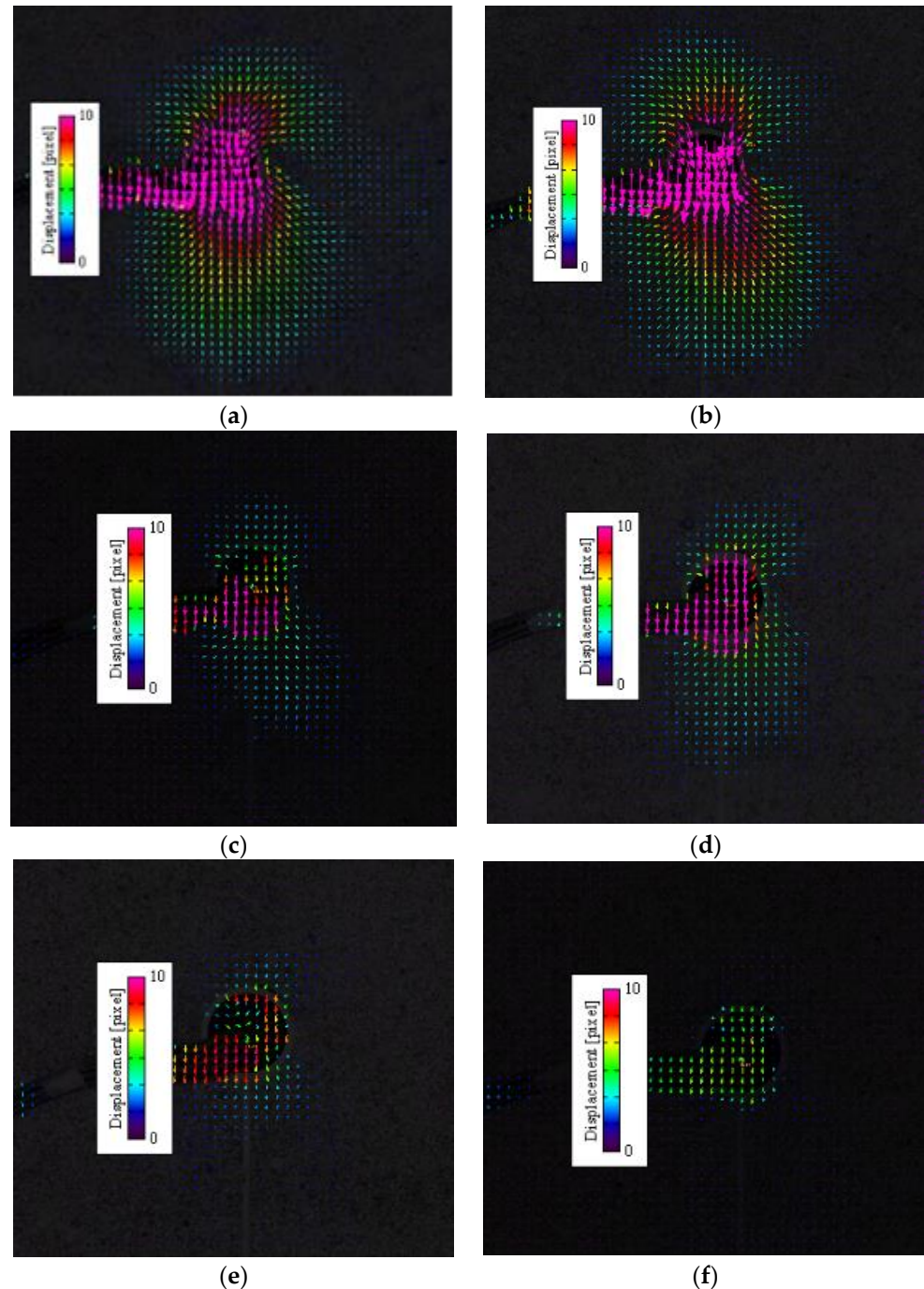


**Figure 6.** PIV image analysis of layered soil test groups under different densities. (a)  $D_r = 0.3$ , the upper small particle size and the lower large particle size; (b)  $D_r = 0.3$ , the upper large particle size and the lower small particle size; (c)  $D_r = 0.5$ , the upper small particle size and the lower large particle size; (d)  $D_r = 0.5$ , the upper large particle size and the lower small particle size; (e)  $D_r = 0.75$ , the upper small particle size and the lower large particle size; (f)  $D_r = 0.7$ , the upper large particle size and the lower small particle size.

Comparing the PIV displacement diagram in Figure 6a,b with the PIV displacement diagram of group A corresponding to 0.3 density, it can be found that the size of the area

affected by the displacement in front of the pile is the largest for single layer coarse sand, followed by the large particle size test group in the upper layer and the small particle size test group in the lower layer, followed by the small particle size test group in the upper layer and the large particle size test group in the lower layer, and the smallest for single layer fine sand. It is not difficult to understand that the stiffness of sand directly affects the displacement of particles under the same load, which is generally characterised by a large stiffness and a small displacement under the same load. In addition, by comparing the PIV image in Figure 6c–f with the PIV image of the single layer sand test group under the corresponding density, it is found that the rules are similar to the comparison results under the above 0.3 density. The stiffness of the upper small particle size and the lower large particle size soil layer is greater than that of the upper large particle size and the lower small particle size soil layer because the mechanical properties of the small particle size sand are better than the large particle size sand. Furthermore, the surface of small particle size sand is more irregular, so its specific surface area is larger. Under the same experimental conditions, the interaction of small particle size sand is stronger than that of large particle size sand.

From Figure 7, it can be seen that under the same horizontal displacement difference, the distance between the displacement isosurfaces is increasing. The overall performance is that the displacement contours in the central area of the pile are dense, and then gradually evacuated with the outward diffusion. In addition, as shown in Figure 7, the displacement contours of each layered soil test group under different densities reflect the influence of sand density on the displacement of soil particles. Comparing Figure 7a,c and Figure 7b,d, as the density increases from 0.3 to 0.5, it can be seen that the maximum distance between the isoline with a displacement of 0.5 mm in front of the pile and the loading centre is decreasing. The maximum distance corresponding to the upper small particle size and the lower large particle size test group is 120 mm under the density of 0.3, and decreases to 97 mm under the density of 0.5. Under 0.3 density, that of the upper large particle size and the lower small particle size test group is 131 mm, while that of 0.5 density is reduced to 101 mm. It can be observed from the above data that, compared with the upper large particle size test group, the upper small particle size soil improves the ability of the soil to resist lateral deformation so that the area reaching the same displacement is narrowed.

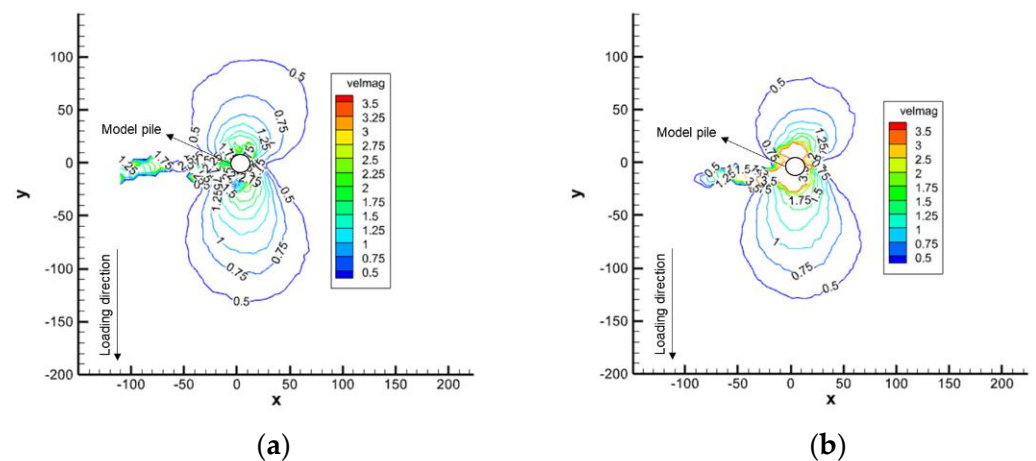
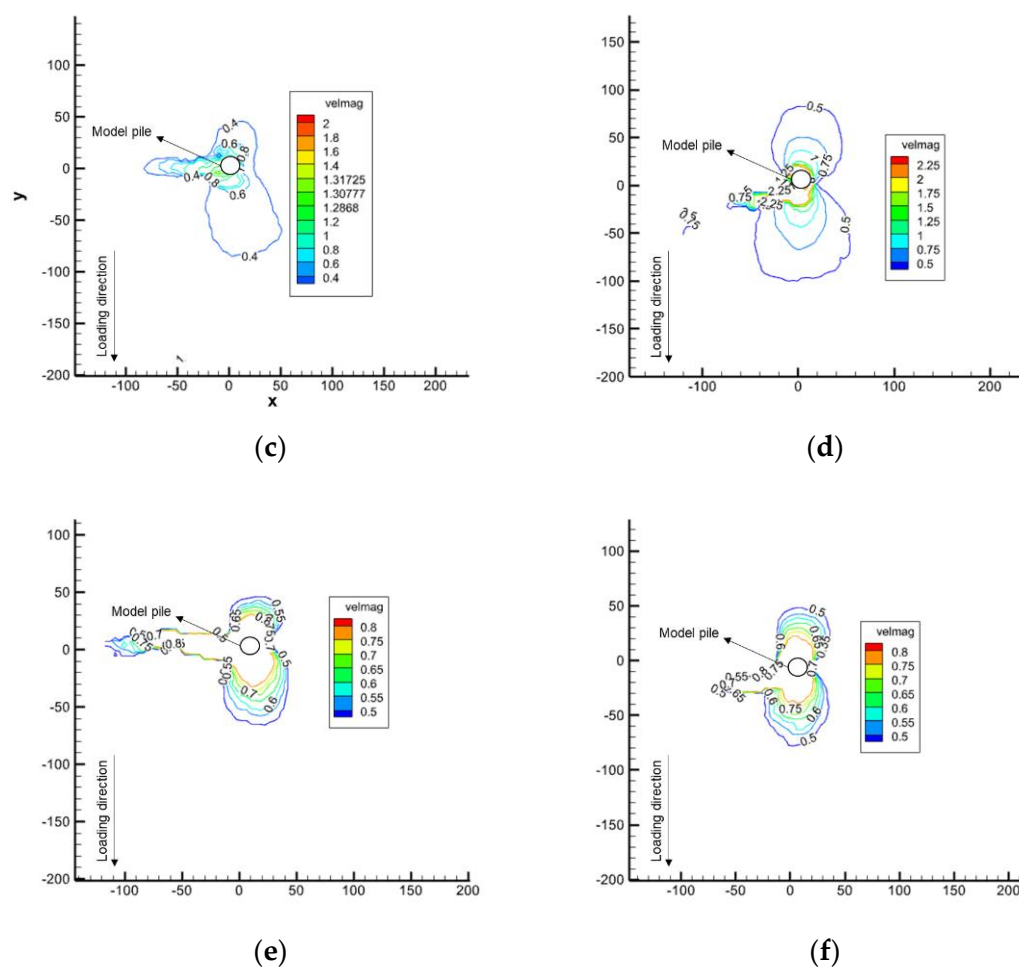


Figure 7. Cont.



**Figure 7.** Displacement field analysis of layered soil test groups with different densities. (a)  $D_r = 0.3$ , the upper small particle size and the lower large particle size; (b)  $D_r = 0.3$ , the upper large particle size and the lower small particle size; (c)  $D_r = 0.5$ , the upper small particle size and the lower large particle size; (d)  $D_r = 0.5$ , the upper large particle size and the lower small particle size; (e)  $D_r = 0.75$ , the upper small particle size and the lower large particle size; (f)  $D_r = 0.7$ , the upper large particle size and the lower small particle size.

In the analysis of the displacement field, the PIV displacement field images of each test group under different compactness are used for statistics on particle movement directions. It is found that the maximum diffusion angle of soil particles in front of the pile is  $45^\circ$ , and the angle has little correlation with the compactness of the soil layer.

## 5. Conclusions

The influence of interlayer soil properties and density on pile–soil interaction were studied through laboratory tests, and the displacement field of the surface soil of horizontally loaded piles was analysed by particle image imaging technology. To be specific, the following conclusions can be drawn from this study:

- (1) The principle and advantages of particle image testing technology were expounded. The combination of particle image testing technology and the pile–soil indoor model test can reduce the influence of data acquisition equipment on model tests and restore the development trend of surface soil displacement in horizontal loading pile test to the greatest extent;
- (2) Through PIV image processing, it can be concluded that under the same horizontal load, the displacement movement trend of the surface soil particles in the single-layer soil and layered soil test group is shown as a spindle-shaped displacement influence

area in front of and behind the pile with the pile body as the centre. However, the maximum angle between the displacement influence area and the horizontal loading direction is little affected by the soil condition and the relative density, and the value is about 45°;

- (3) Using PIV technology and Tecplot for quantitative analysis, it is found that, with the increase of density in different experimental groups, the influence area of soil displacement behind the pile and in front of the pile gradually decreased. It can also be concluded that the order of soil stiffness from small to large is: single layer coarse sand, upper large particle size lower and small particle size test group, upper small particle size and lower large particle size test group, single layer fine sand.

**Author Contributions:** Conceptualization, X.Z. and H.L.; methodology, X.Z.; software, H.L.; validation, X.Z., H.L. and K.X.; formal analysis, H.L.; investigation, Z.M.; resources, Y.W.; data curation, R.Y.; writing—original draft preparation, X.Z.; writing—review and editing, K.X.; visualization, X.Z.; supervision, H.L.; project administration, K.X. All authors have read and agreed to the published version of the manuscript.

**Funding:** This research received no external funding.

**Data Availability Statement:** The data presented in this study are available upon request from the corresponding author.

**Conflicts of Interest:** The authors declare no conflict of interest.

## References

1. Reese, L.; Cox, W.; Koop, F. Analysis of laterally loaded piles in sand. In Proceedings of the 6th Offshore Technology Conference, Houston, TX, USA, 5–7 May 1974; Volume 2.
2. Matlock, H. Correlation for design of laterally loaded piles in soft clay. In Proceedings of the 2nd Offshore Technology Conference, Houston, TX, USA, 21–23 April 1970; Volume 1.
3. Murchison, J.; O’neill, M. Evaluation of p-y relationships in cohesionless soils. *Proc. Anal. Des. Pile Found.* **1984**, *3*, 174–191.
4. Mayne, P.W. Laboratory modeling of laterally-loaded drilled shafts in clay. *J. Geotech. Eng.* **1995**, *121*, 827–835. [[CrossRef](#)]
5. Lianyang, Z.; Zhuchang, C. Model test of laterally loaded piles in cohesive soil. *Chin. J. Geotech. Eng.* **1990**, *12*, 40–50.
6. Di, C.; Qing, R.; Yang, L.; Chao, Y.; Zhe, K. Study on mechanical behavior of piles in sand and clay under lateral load. *J. Water Resour. Water Eng.* **2016**, *27*, 212–216.
7. Alderlieste, E.A. Experimental modelling of lateral loads on large diameter mono-pile foundations in sand. In Proceedings of the 30th International Conference on Ocean, Offshore and Arctic Engineering, Rotterdam, The Netherlands, 19–24 June 2011; pp. 126–138.
8. Yuan, B.; Chen, W.; Zhao, J.; Li, L.; Liu, F.; Guo, Y.; Zhang, B. Addition of alkaline solutions and fibers for the reinforcement of kaolinite-containing granite residual soil. *J. Appl. Clay Sci.* **2022**, *228*, 106644. [[CrossRef](#)]
9. Yuan, B.; Chen, W.; Li, Z.; Zhao, J.; Luo, Q.; Chen, W.; Chen, T. Sustainability of the polymer SH reinforced recycled granite residual soil: Properties, physicochemical mechanism, and applications. *J. Soils Sediments* **2022**, 1–17. [[CrossRef](#)]
10. White, D.J.; Take, W.A.; Bolton, M.D. Soil deformation measurement using particle image velocimetry (PIV) and photogrammetry. *Geotechnique* **2003**, *53*, 619–631. [[CrossRef](#)]
11. Stanier, S.A.; Blaber, J.; Take, W.A.; White, D.J. Improved image-based deformation measurement for geotechnical applications. *Can. Geotech. J.* **2016**, *53*, 727–739. [[CrossRef](#)]
12. Yuan, B.; Chen, M.; Chen, W.; Luo, Q.; Li, H. Effect of Pile-Soil Relative Stiffness on Deformation Characteristics of the Laterally Loaded Pile. *Adv. Mater. Sci. Eng.* **2022**, *2022*, 4913887. [[CrossRef](#)]
13. Ting, H.; Guoliang, D.; Weiming, G.; Jinhai, Z.; Guoping, X. Application of particle image velocimetry in model test of negative friction of pile foundations. *Geotech. Mech.* **2013**, *34* (Suppl. S1), 162–166+172. [[CrossRef](#)]
14. Xuan, W.; Xinli, H.; Chang, Z.; Lanxing, L. Variation characteristics of displacement field of landslide-anti-slide pile based on physical model test. *Geol. Sci. Technol. Bull.* **2020**, *39*, 103–108. [[CrossRef](#)]
15. Wenxue, W.; Lingyu, S.; Jingyuan, X.; Qingyang, H.; Tong, J. Experiment on compression-shear failure characteristics of rock mass with through single fracture based on PIV technology. *J. Eng. Geol.* **2021**, *29*, 1121–1130. [[CrossRef](#)]
16. Yuan, B.; Sun, M.; Xiong, L.; Luo, Q.; Pradhan, S.P.; Li, H. Investigation of 3D deformation of transparent soil around a laterally loaded pile based on a hydraulic gradient model test. *J. Build. Eng.* **2020**, *28*, 101024. [[CrossRef](#)]
17. Yuan, B.; Li, Z.; Zhao, Z.; Ni, H.; Su, Z.; Li, Z. Experimental study of displacement field of layered soils surrounding laterally loaded pile based on Transparent Soil. *J. Soils Sediments* **2021**, *21*, 3072–3083. [[CrossRef](#)]
18. Yuan, B.; Chen, W.; Zhao, J.; Yang, F.; Luo, Q.; Chen, T. The Effect of Organic and Inorganic Modifiers on the Physical Properties of Granite Residual Soil. *Adv. Mater. Sci. Eng.* **2022**, *2022*, 9542258. [[CrossRef](#)]

19. GB/T 50123-2019; Standard for Soil Test Methods. Ministry of Housing and Urban-Rural Development of the People's Republic of China: Beijing, China, 2019.
20. Bingxiang, Y.; Meng, S.; Yixian, W.; Lihua, Z.; Qingzi, L.; Xuqun, Z. Full 3D displacement measuring system for 3D displacement field of soil around a laterally loaded pile in transparent soil. *ASCE Int. J. Geomech.* **2019**, *19*, 04019028. [[CrossRef](#)]
21. Yuan, B.; Li, Z.; Chen, W.; Zhao, J.; Lv, J.; Song, J.; Cao, X. Influence of Groundwater Depth on Pile–Soil Mechanical Properties and Fractal Characteristics under Cyclic Loading. *Fractal Fract.* **2022**, *6*, 198. [[CrossRef](#)]